Geological Quarterly, 2021, 65: 7
DOI: http://dx.doi.org/10.7306/gq.1572

A rare indium-bearing mineral (Zn-In-Cu-Fe sulphide) from the Stara Kamienica Schist Belt (Sudetes, SW Poland)

Rafał MAŁEK[1, *] and Stanisław Z. MIKULSKI[1]

[1] Polish Geological Institute – National Research Institute, Rakowiecka 4, 00-975 Warszawa, Poland

Małek, R., Mikulski, S.Z., 2021. A rare indium-bearing mineral (Zn-In-Cu-Fe sulphide) from the Stara Kamienica Schist Belt (Sudetes, SW Poland). Geological Quarterly, 2021, 65: 7, doi: 10.7306/gq.1572

A rare indium-bearing mineral from the stratiform Czerniawa Zdrój-Krobica Sn deposit in the Sudetes (NE part of the Bohemian Massif) has been recognized in the qualitative-quantitative chemical composition studies of sulphide-cassiterite samples by electron microprobe (EMPA). This indium-bearing mineral occurs in the form of separate hipautomorphic microscopic grains (diameter 5–20 μm) and as intergrowths and disseminations in chalcopyrite. Observations indicate that this phase crystallized with the main generation of chalcopyrite, sphalerite and also with a younger generation of cassiterite in the mineral succession. The chemical composition of this mineral is as follows: S – 29.38–30.77 wt.%, Zn – 29.76–34.02 wt.%, In – 17.52–19.40 wt.%, Cu – 9.05–10.75 wt.%, Fe – 7.76–8.7 wt.% and Sn – 0.03–0.1 wt.%. Its calculated chemical formula is: $(Zn_{2.09}In_{0.67}Cu_{0.65}Fe_{0.64}Cd_{0.02})_{\Sigma 4.07}S_{4.0}$ and it is characterized by enrichment of Zn with simultaneous depletion in Cu and Sn relative to the ideal chemical composition of sakuraiite – the most similar mineral in terms of chemical composition. In the light of our new data, it should be considered as a yet unnamed Zn-In-Cu-Fe sulphide mineral. In addition, coexisting sulphide minerals – chalcopyrite (max. 1580 ppm of In) and sphalerite (max. 1640 ppm of In) were identified as indium carriers.

Key words: indium mineral, sulphide-cassiterite ore, Sn deposit, Sudetes.

INTRODUCTION

Indium occurrences in Poland have been recognized in stratiform tin deposits of the Stara Kamienica Schist Belt in the West Sudetes (Foltyn et al., 2020 and references therein) and within Zn-Pb ores hosted by Triassic carbonates of the Upper Silesia Coal Basin boundary (Mikulski et al., 2020a, and references therein). An indium-bearing mineral phase present in the cassiterite-sulphide mineralization of the Stara Kamienica Schist Belt had been previously recognized during trace and critical element studies in this area (Mikulski et al., 2018). Based on preliminary EMPA results, this mineral was referred to as sakuraiite, but there was too little data for accurate identification. Accordingly, additional work has been undertaken, involving more detailed EMPA studies. They were focused on extending the set of analysed elements, measuring chemical composition on as many mineral grains and places of occurrence of this indium-bearing mineral as possible and increasing the sensitivity of EMPA measurements by applying a higher beam current (40 nA) and using different In standards (InAs and InSb). In this paper we provide results of EMPA analyses performed on a *Cameca SX-100* electron probe, leading to more detailed characterization and identification of this indium-bearing mineral.

OVERVIEW OF INDIUM MINERALOGY

The main carriers of indium are zinc, copper, iron and tin sulphides (mainly sphalerite, chalcopyrite, stannite) and tin oxide (cassiterite) (Stevens and White, 1990; Schwarz-Schampera and Herzig, 2002; Schwarz-Schampera, 2014; Pavlova et al., 2015; Frenzel et al., 2016; Sahlström et al., 2017). In base metal sulphides indium replaces elements with similar ionic radius showing a tendency for substitution in a molecule with tetrahedral geometry (Schwarz-Schampera and Herzig, 2002). Incorporation of indium into sulphide structures can occur due to substitution of copper, iron, tin and arsenic in the crystal structure and also by forming submicroscopic inclusions of indium minerals within sulphides. Crystallization of indium-bearing sulphides can be caused by both primary precipitation from hydrothermal fluids and also as a result of remobilization and recrystallization in the hydrothermal zone through thermal metamorphism (Schwarz-Schampera and Herzig, 2002). Indium remains in melt during magma crystallization until a late stage. The indium content of rock-forming minerals is usually low, but increased concentrations are present in some mafic and ultramafic rocks, e.g. peridotite, komatiite, basalt and dolerite; studies show that slight indium enrichment can be found in

* Corresponding author, e-mail: rafal.malek@pgi.gov.pl

Received: May 5, 2020; accepted: November 9, 2020; first published online: December 29, 2020

more fractionated Fe-rich pyroxenes (Wager et al., 1958). Indium barely incorporates into most rock-forming minerals that crystallize from felsic magmas. The average content of indium in continental crust is 0.05 ppm and in oceanic crust it is 0.072 ppm (Taylor and McLennan, 1985).

Indium shows chalcophile preferences and rarely forms its own minerals – so far 13 indium minerals have been identified and characterized (including native indium). The occurrence of native indium was discovered for the first time by Ivanov (1963), while Nechayev (1987) identified native indium within tin mineralization on the Ukrainian Shield.

The most significant and most common indium minerals are roquesite [$CuInS_2$], dzhalindite [$In(OH)_3$], indite [$Fe^{2+}In_2S_4$], laforetite [$AgInS_2$] and sakuraiite [$(Cu,Zn,Fe,Ag)_3(In,Sn)S_4$] (Genkin and Murav'eva, 1963; Picot and Pierrot, 1963; Cantinolle at al., 1985; Schwarz-Schampera and Herzig, 2002). Sakuraiite was discovered by Kato (1965) in polymetallic vein-type mineralization of the Ikuno deposit (central Japan). It was found in altered Cretaceous felsic tuffs within a fine grained sulphide association of stannite, cassiterite and sphalerite. EMPA studies indicated that the metal contents are variable and show the following tendency: Cu>Zn>Fe>Ag and In>Sn with different substitution configurations (Shimizu et al., 1986). The average chemical composition of sakuraiite is given in Table 1 (after Anthony et al., 1990) and its empirical formula is: $(Cu_{1.4}Zn_{0.9}Fe^{2+}_{0.4}Ag_{0.1})(In_{0.9}Sn_{0.1})S_4$.

INDIUM OCCURRENCE IN VARIOUS DEPOSIT TYPES AND ITS RESOURCES

There is no official data regarding global indium resources (Anderson, 2020) but estimates suggest ~50,000.0 tons (proved and probable, of which proved resources constitute ~15,000.0 tons in 2013; (Lokanc et al., 2015), while the annual production of this metal is ~760 tons (in 2019). Indium is necessary for the production of high purity alloys in metallurgy, LCD panels (liquid crystal displays), touch screens used in modern electronic devices and for manufacturing solar panels (Jorgenson and George, 2005; Torró et al., 2019). Statistical analysis of the indium content in polymetallic deposits indicates that the highest concentrations of this metal occur in chalcopyrite ore which contains almost twice as much indium as sphalerite ore (Ivanov, 1963; Schwarz-Schampera and Herzig, 2002). Despite this, sphalerite remains the most important indium carrier as In production is based on zinc concentrates. Three main indium-enriched metallogenic provinces have been recognized:

- the subduction zone of the western edge of the Pacific plate (SE Asia in particular);
- the edge of the Nazca and South American plates (especially in Bolivia and Peru);
- metallogenic areas of central Europe (connected with the Variscan and Alpine orogenies; Schwarz-Schampera and Herzig, 2002);
- In addition, other areas containing mineralization with lower indium contents were also identified, such as the Appalachian Mountains in North America and greenstone belts in Canada and South Africa.

Indium occurs in different deposit types, mainly within magmatogenic ore deposits (porphyry type deposits, skarn deposits, pegmatites and granite-related deposits, epithermal Ag-Au deposits, volcanogenic massive sulphide deposits), sedimentary exhalative related ore deposits and hydrothermal ore deposits (stratiform sediment-hosted deposits and MVT deposits) (Schwarz-Schampera and Herzig, 2002; Dill, 2010). In each of these deposit types, indium occurs in different mineral associations and parageneses. In most cases it coexists with base metals e.g. Cu, Sn, Zn, Pb, As, Fe but also with other metals – Bi, Co, Ag and W (Schwarz-Schampera and Herzig, 2002).

In stockwork-vein Sn-W deposits and porphyry Sn deposits, indium concentrations are associated with post-collisional granitic intrusions, especially with centres of subvolcanic polyphase intrusions and related magmatic hydrothermal activity. The indium mineralization is associated with fractures, veinlets, and disseminations of late-stage polymetallic tin-base metal mineralization which display complex associations of copper-tin-bismuth-lead-silver-arsenic-dominated minerals (Schwarz-Schampera and Herzig, 2002). Both the Sn-W vein-stockwork and Sn porphyry deposits are important sources of indium accumulations, e.g. the Mount Pleasant deposit (New Brunswick, Canada) contains ~25% of proved indium global reserves (Kooiman and Ruitenberg, 1992).

Volcanogenic massive sulphide (VMS) deposits, both Archean and presently-forming ores of actively-spreading ridges on the modern seafloor, are also an important source of indium. Large-scale copper-zinc massive sulphide deposits usually show a close metallogenic association of indium with the copper-rich, high-temperature element suite. Indium-bearing VMS deposits occur in submarine, bimodal volcanic sequences of palaeo-trench structures and rift basins and they are closely associated with calc-alkaline rhyodacite to rhyolite flows and

Table 1

Chemical composition of sakuraiite (wt.%; after Anthony et al., 1990)

Element	Chemical composition of 3 sakuraiites (after Anthony et al.,1990)			Average chemical composition from 3 sakuraiites provided by Anthony et al. (1990)	Chemical composition of sakuraiite (after webmineral.com)
Zn	14.0	13.7	18.0	15.2	13.9
In	23.0	22.0	23.8	22.9	24.4
Fe	5.0	6.9	4.5	5.5	5.3
Cu	21.0	19.6	18.9	19.8	21.0
Ag	3.5	0.2	0.1	1.3	2.5
Sn	4.0	7.2	4.9	5.4	2.8
Cd	–	0.6	0.7	0.7	–
S	30.0	29.1	29.0	29.4	30.2
Sum	100.5	99.3	99.9	99.9	100.0

volcanoclastic rocks. Deposits enriched in indium usually also contain elevated contents of silver, lead, tin, cobalt, bismuth, and selenium while they are depleted in gold.

In the epithermal environment, indium mineralization dominates in base metal-rich deposits of the low-sulphidation subtype. Mineralizations containing indium are usually connected with rhyolite, dacite and andesite volcanism. Indium mineralization is related to the late-stage, high- to medium-temperature (380–250°C) deposition of the copper-silver-tin-arsenic-lead association from acidic to near neutral and reduced environments. Indium-bearing fluids have a heterogeneous source with mixing between high-temperature magmatic fluids and meteoric water (Schwarz-Schampera and Herzig, 2002).

OCCURRENCE OF INDIUM IN THE TIN DEPOSITS OF THE STARA KAMIENICA SCHIST BELT

Indium has been recognized in the Sudetes within the tin mineralization of the Stara Kamienica Schist Belt by various authors (Wiszniewska, 1984; Piestrzyński and Mochnacka, 2003; Mikulski et al., 2018; Mikulski and Małek, 2019; Małek et al., 2019; Foltyn et al., 2020). This schist belt, belonging to the Karkonosze-Izera-Lausitz Block, is a part of the Izera Metamorphic Complex (called also the northern cover of the Karkonosze granite intrusion) within which there are five longitudinally extended schist belts (Fig. 1; Smulikowski, 1972; Mazur et al., 2006; Mochnacka et al., 2015). The largest one, the Stara Kamienica belt, is composed of two main rock complexes. The first is represented by gneisses, granite-gneisses and pre-Variscan granites while the second one consists of quartz-chlorite-mica schists with variable proportions of individual minerals (Szałamacha and Szałamacha, 1974; Michniewicz et al., 2006). Some parts of the schists contain cassiterite-sulphide mineralization (Fig. 2).

The mica schists in which the cassiterite-sulphide mineralization occurs are fine-grained rocks with lepidoblastic or granoblastic texture, light grey or silver-grey colour (in places with a greenish tint) and with visible foliation and lamination. The main rock-forming minerals are quartz and muscovite with chlorite, biotite, garnet and albite (Szałamacha and Szałamacha, 1974). Tin-bearing schists have thickness from 50 to 180 m and lie between packets of barren schists from which they differ in higher amounts of biotite, garnet, chlorite and by an elevated content of iron (Michniewicz et al., 2006 with references therein). Within the schists there are quartz lenses, folds and veinlets locally containing chlorite, calcite and fluorite (Michniewicz et al., 2006).

The main ore mineral occurring in the Izera tin mineralization is cassiterite (SnO_2) which appears in the schists as small (max. 300 μm, usually up to 100 μm across) hipautomorphic or rarely automorphic grains forming grape-like concentrations in association with quartz, chlorite and less often with sulphides, muscovite and biotite (Szałamacha and Szałamacha, 1974;

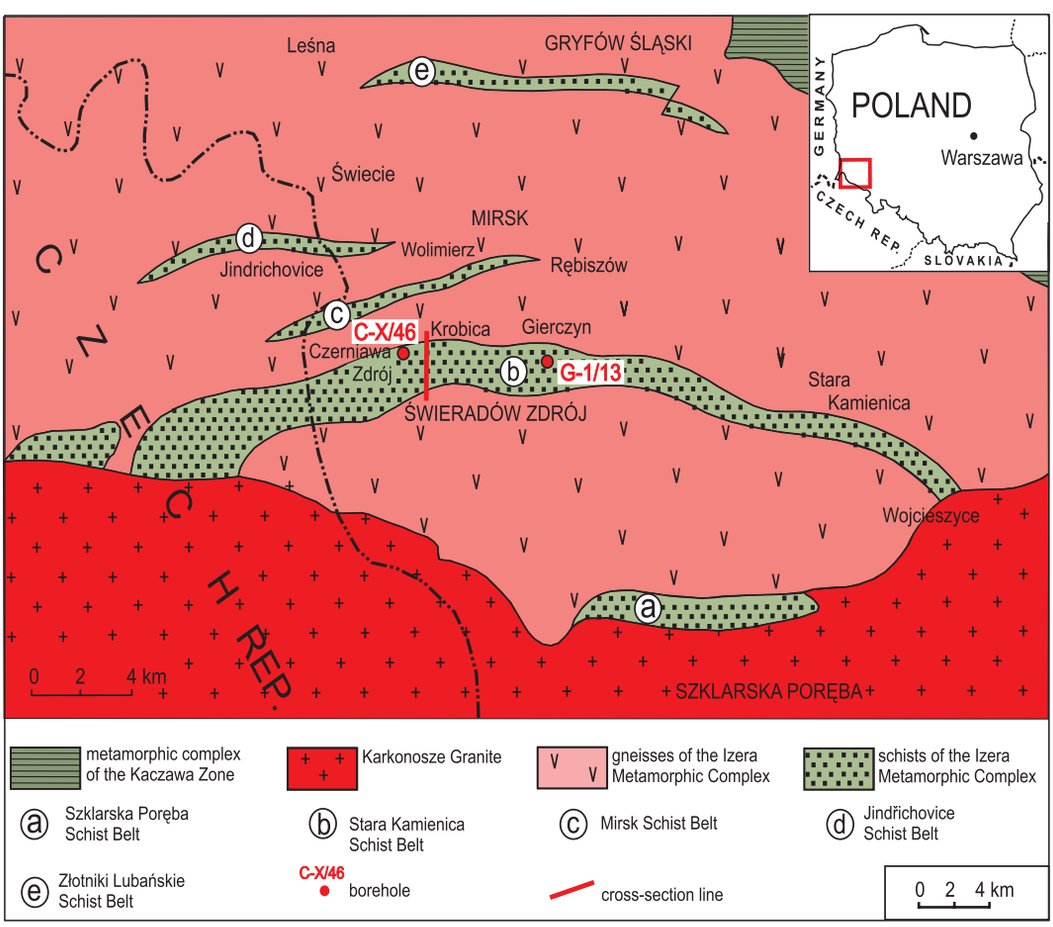

Fig. 1. Schematic geological map of the Stara Kamienica Schist Belt (after Michniewicz et al., 2006) with the location of the boreholes from which samples were subjected to EPMA research

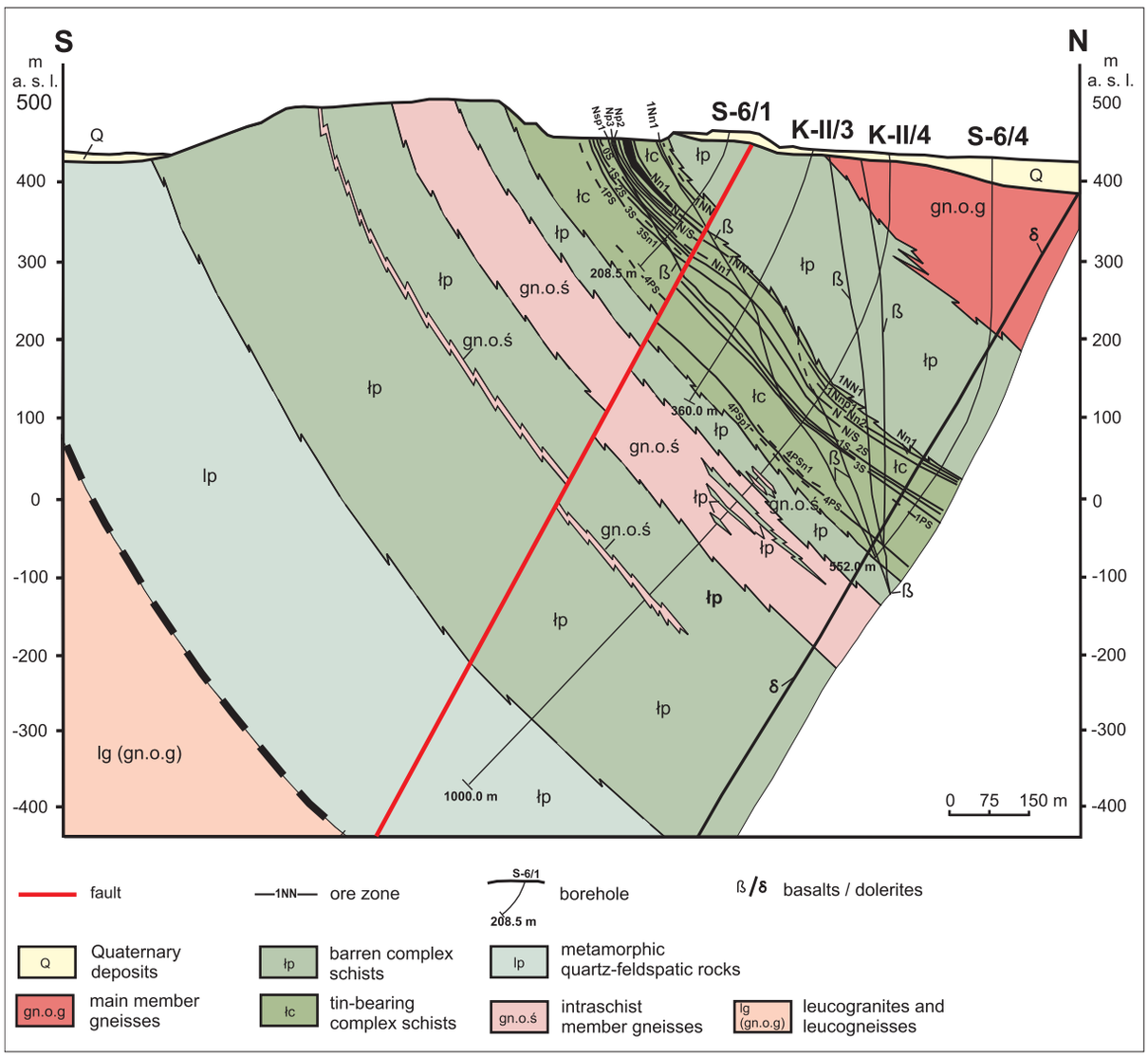

Fig. 2. Geological cross-section through the Stara Kamienica Schist Belt with tin mineralization (modified after Michniewicz et al., 2006)

Kowalski et al., 1978; Wiszniewska, 1983, 1984; Mochnacka, 1986; Berendsen et al., 1987; Kucha and Mochnacka, 1987; Kozłowski et al., 1988; Bobiński, 1991; Piestrzyński et al., 1990, 1992; Cook and Dudek, 1994; Michniewicz et al., 2006; Mochnacka et al., 2015; Mikulski et al., 2018). In addition, it is observed as intergrowths in almost every rock-forming mineral (including garnets) (Wiszniewska, 1984; Bobiński, 1991).

Base metal sulphides present in the mineralized zones are usually easy to identify macroscopically, however, they are not restricted to the zones mineralized with tin, as they form an individual mineral association (Wiszniewska, 1984; Berendsen et al., 1987 Cook and Dudek, 1994; Piestrzyński and Mochnacka, 2003; Mikulski et al., 2018). The sulphides occur within schist laminae or quartz clusters and they are mainly represented by pyrrhotite, chalcopyrite, arsenopyrite, sphalerite, galena, pyrite and less common bismuthinite. In total, over a dozen ore minerals co-occurring with cassiterite mineralization have been identified. This mineral association is referred to a quartz-chlorite-sulphide tin deposit (Wiszniewska, 1984).

METHODS

Samples taken from the Czerniawa C-X/46 and Gierczyn G-1/13 archival boreholes were examined in the Polish Geological Institute – National Research Institute as part of a project aimed to quantitatively and qualitatively identify trace elements in various metallogenic deposits in Poland (Mikulski et al., 2018). Chemical analyses in accordance with standard procedures were carried out in the Chemical Laboratory of the Polish Geological Institute – National Research Institute in the period

2016–2018. Indium, like most of the trace elements from rock samples of the Stara Kamienica Schist Belt, was determined by Inductively Coupled Plasma Mass Spectrometry (ICP-MS) (see Mikulski et al., 2020a for the method applied). The lowest detection limit of indium ICP-MS method determination was 0.05 ppm (Mikulski et al., 2020a).

Detailed mineralogical and petrological investigation with photographic documentation of the cassiterite-sulphide mineralization was carried out on a *NICON ECLIPSE LV100 POL* microscope with *NIS-Elements* software while quantitative measurements were made using an electron microprobe (EMPA) *CAMECA SX-100,* preceded by preliminary studies using an electron microscope *LEO-1430 (ZEISS)* with EDS detector. Chemical composition of ore minerals in micro-areas, using WDS spectrometers, was determined with the following parameters: acceleration voltage HV - 15 kV; beam current 40 nA; focused beam (<1 μm in diameter); the international (commercial) standards used were from the SPI-53 set from SPI and from the sulf-16 set from P&H: Cu, S, Fe – chalcopyrite; Au – Au metal.; Co, As – skutterudite; Sb – stibnite Sb_2S_3; Ni – Ni metal.; Zn – ZnS synt.; Pb – galena; Hg – cinnabar HgS; Cd – CdS synt.; Ag – hessite Ag_2Te; In – InAs and InSb; Sn – cassiterite SnO_2; Ga – Ga_2Se_3; As – arsenopyrite.

RESULTS

INDIUM IN GEOCHEMICAL INVESTIGATION

Elevated concentrations of indium were identified in core samples taken from the archival boreholes (Fig. 1) of documented tin deposits in Krobica, Gierczyn and Krobica Zachód – Czerniawa (Mikulski et al., 2018). Geochemical investigation of 42 samples using ICP-MS indicated minimum In content below detection limit (which is 0.05 ppm) and maximum of 7.42 ppm (Mikulski et al., 2018). The arithmetic mean of In is 0.93 ppm and geometric mean is 0.41 ppm. Indium shows positive correlation with copper (correlation coefficient r = 0.79, Fig. 3A), weak correlation with gold (r = 0.50) and very weak with zinc (Fig. 3B), uranium, bismuth (r = 0.42), chromium, cobalt and silver.

The average indium content in Earth's crust is 0.049 ppm (Barbalace, 2019) while chemical data of tin-bearing samples from the Stara Kamienica Schist Belt shows an In geometric mean of 0.41 ppm (median = 0.42 ppm) which indicates >8-times enrichment in comparison to the crustal abundance of indium (in the case of the arithmetic mean of 0.92 ppm, >18-times enrichment).

INDIUM-BEARING MINERALS

INDIUM IN CHALCOPYRITE

Several grains of chalcopyrite up to 2 mm across were investigated for indium content. Chalcopyrite forms xenomorphic grains and often occurs as sulphide aggregates mainly with pyrite, pyrrhotite and less often with arsenopyrite, sphalerite or bismuthinite. Chalcopyrite commonly contains inclusions of other minerals, mostly sulphides such as sphalerite, bismuthinite and also cassiterite and native bismuth. It also appears in the form of intergrowths in other sulphide minerals or in cracks within garnets (Fig. 4A–C).

A total of 56 WDS points were measured within chalcopyrite grains. The results showed an indium content ranging from <149 ppm (detection limit) up to a maximum content of 1580 ppm. Most (40 of 56) measurements showed an indium content above the detection limit, the arithmetic mean being 330 ppm.

The average chemical composition of the chalcopyrite is 34.45 wt.% Cu, 29.99 wt.% Fe and 34.47 wt.% S (Table 2). Figure 4D presents a WDS spectrum of chalcopyrite with visible peaks of indium, cadmium and iron. Figure 4C shows some of the chalcopyrite grains with WDS points marked, the results of which are shown in Table 2.

INDIUM IN SPHALERITE

Sphalerite occurs occasionally and much less often than chalcopyrite in the samples studied. It co-creates sulphide aggregates of hydrothermal origin in which there are xenomorphic grains (Fig. 5A–C). Sphalerite usually occurs as intergrowths in chalcopyrite and pyrrhotite. Chemical composition analyses for indium admixtures were made on seven sphalerite grains with 21

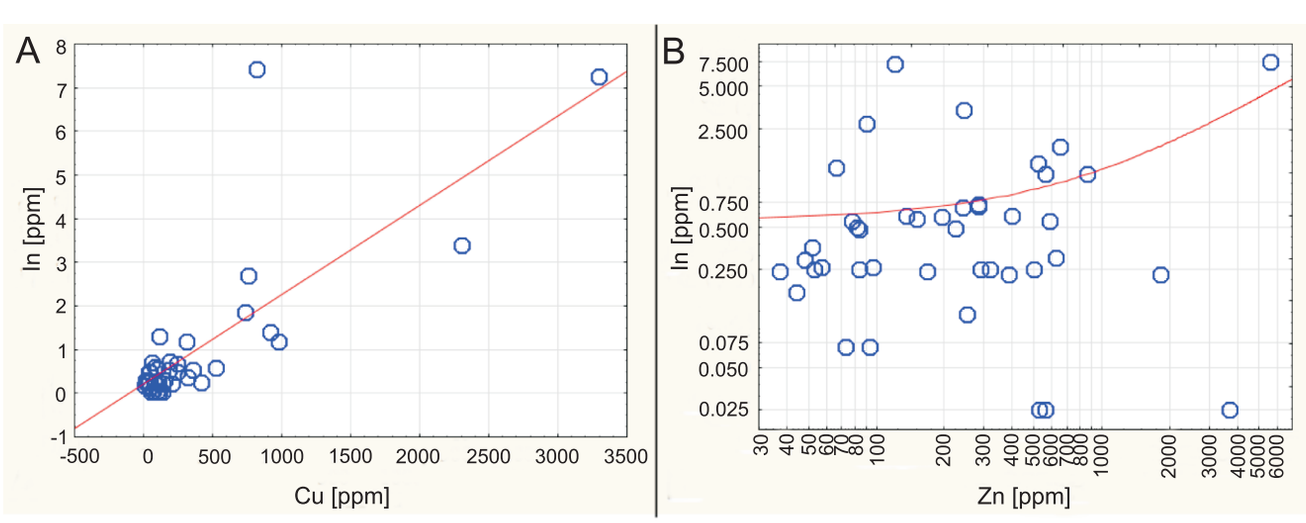

Fig. 3. Correlation chart of In *versus* Cu (A) and In *versus* Zn (B) with marked trend lines from samples of cassiterite-sulphide mineralization (Stara Kamienica Schist Belt, Sudetes; after Mikulski et al., 2018)

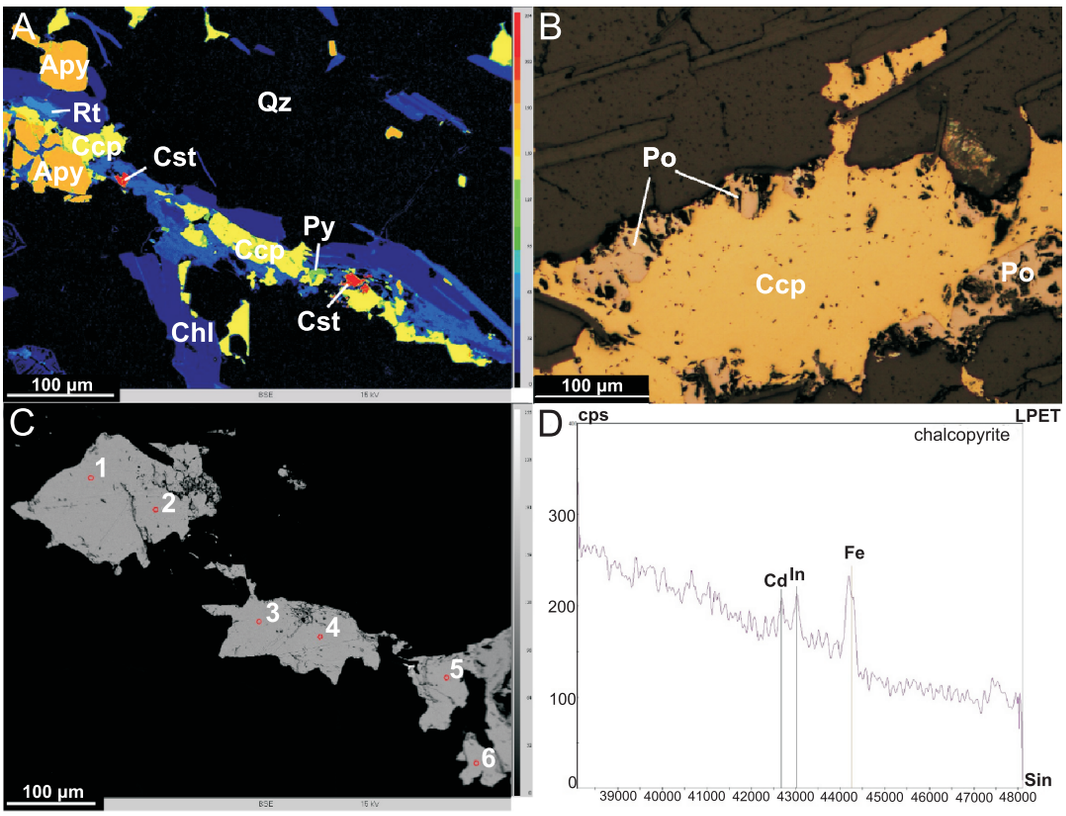

Fig. 4. The cassiterite (2nd generation) – sulphide association within quartz-chlorite schist from the C-X/46 borehole (depth 235.5 m)

A – cassiterite (Cst) – aggregate of chalcopyrite (Ccp), rutile (Rt), pyrite (Py) and arsenopyrite (Apy) within quartz (Qz) – chlorite (Chl) schist, BSEI (Backscattered Electron Image); **B** – chalcopyrite with pyrrhotite (Po), reflected light; **C** – BSEI of chalcopyrite grains with measurement points; **D** – WDS spectrum of chalcopyrite with peaks of indium, cadmium and iron marked

Table 2

WDS results of the measurement points in chalcopyrite from Figure 4C

Point#	S [wt.%]	Cu [wt.%]	Fe [wt.%]	Si [ppm]	Ag [ppm]	Pb [ppm]	Zn [ppm]	Ni [ppm]	Co [ppm]	Au [ppm]	Ba [ppm]	Ga [ppm]	In [ppm]	Total
1	34.34	34.38	30.23	260	160	b.d.l.	910	320	330	240	610	350	400	99.4
2	34.47	34.68	30.3	240	170	b.d.l.	b.d.l.	b.d.l.	380	1080	100	140	470	99.8
3	34.57	34.5	30.23	220	590	550	1290	500	540	690	b.d.l.	90	710	99.84
4	34.84	34.52	30.27	360	520	280	b.d.l.	600	640	b.d.l.	1350	b.d.l.	680	100.1
5	34.58	34.03	30.36	230	450	390	660	280	440	b.d.l.	1110	230	540	99.5
6	35.24	34.34	29.77	410	620	b.d.l.	1070	b.d.l.	550	790	570	170	510	99.92

Al, Te, Ca, Cd, Cl, Sb, Bi, Se, As, Mg and Mo below detection limits; b.d.l. – below detection limit

WDS measuring points. The results showed an indium content ranging from less than 154 ppm (detection limit) up to a maximum of 1640 ppm. Indium was only not detected in one analysed spot and the arithmetic mean of In content in the rest of the points is 380 ppm (n = 20). The average measured chemical composition of sphalerite is 57.4 wt.% Zn, 8.1 wt.% Fe and 32.6 wt.% S. In addition, high concentrations of some elements have been noted: Cd (mean 5570 ppm), Cu (mean 3720 ppm), Ga (mean 1001 ppm) and Co (mean 580 ppm). Figure 5D presents a WDS spectrum of sphalerite with visible peaks of indium, cadmium and iron. Figure 5C shows a sulphide aggregate containing sphalerite with measurement points indicated (results in Table 3).

INDIUM-BEARING MINERAL

The Indium-bearing mineral (IBM), which is a Zn-In-Cu-Fe sulphide, has been identified so far only in one sample taken from 223.6 m depth of the C-X/46 archival borehole and it occurs in the form of separate hipautomorphic grains, 5 to ~20 µm in size and as intergrowths in chalcopyrite (also with diameter up to 20 µm; Fig. 6). In addition, backscattered electron image (using higher contrast) shows that indium-bearing mineral grains have homogeneous internal structure.

A total of 7 WDS measurement points were selected on 6 grains of the Zn-In-Cu-Fe sulphide (two occurring as inter-

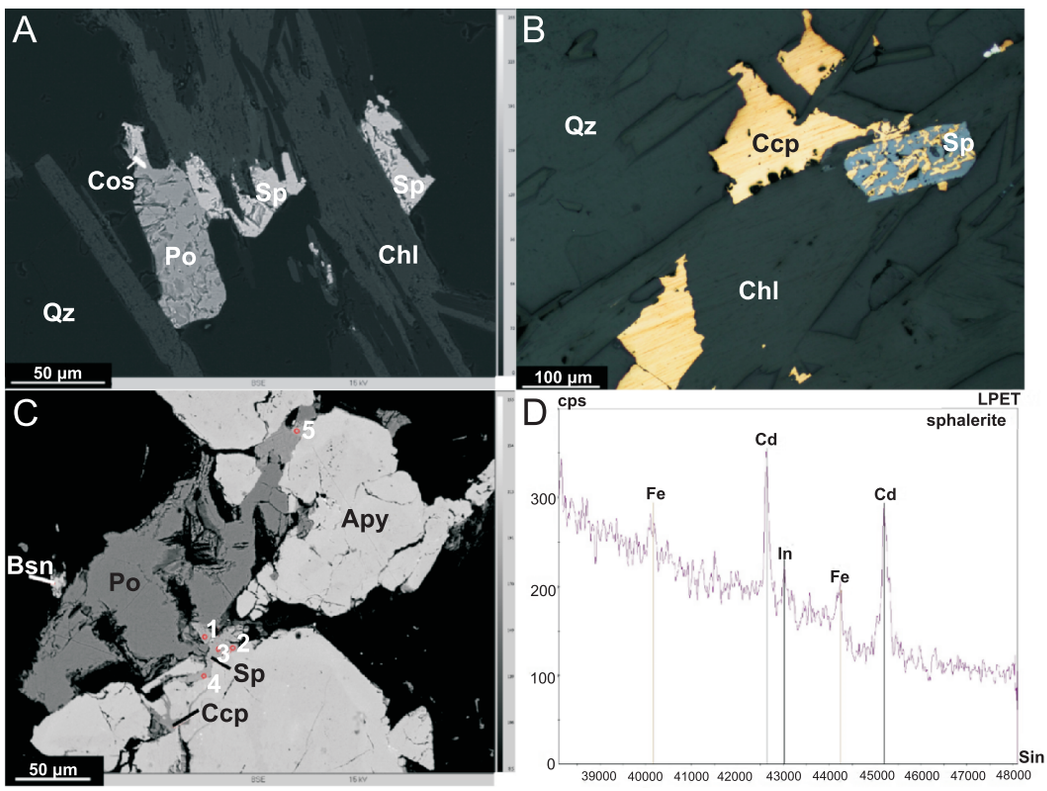

Fig. 5. Examples of sphalerite occurrences in sulphide aggregates, borehole G-1/13, depth 158.5 m

A – sulphide aggregate within chlorite (Chl) lamina consisting of pyrrhotite (Po) with costibite intergrowth [CoSbS] (Cos) and sphalerite (Sp), BSEI; **B** – chalcopyrite (Ccp)-sphalerite (Sp) aggregate on the edge of quartz (Qz) and chlorite (Chl) laminae, reflected light; **C** – sulphide aggregate consisting of pyrrhotite (Po) – arsenopyrite (Apy) – chalcopyrite (Ccp) – sphalerite (Sp) with bastnäsite [$Ce(CO_3)F$] (Bsn) with WDS measuring points on sphalerites marked, BSEI; **D** – WDS spectrum of sphalerite with peaks of indium, cadmium and iron marked

Table 3

WDS results of the measurement points in sphalerite from Figure 5C

Point#	S [wt.%]	Zn [wt.%]	Fe [wt.%]	Si [ppm]	Cd [ppm]	Cu [ppm]	Co [ppm]	Ga [ppm]	In [ppm]	Total
1	33	57.23	8.07	90	8820	480	760	1070	230	99.59
2	32.87	56.21	7.6	480	7820	10660	1550	980	310	99.18
3	32.92	57.11	7.86	290	8570	670	1170	940	170	99.14
4	32.61	57.14	7.51	130	8820	4830	1450	940	220	99.11
5	33.13	56.47	8.24	270	7660	5420	1060	1140	170	99.63

Al, Ca, Cl, Ag, Te, Sb, Bi, Ni, Pb, Se, As, Mg, Au, and Ba below detection limits

growths in chalcopyrite and four as separate ones) and their results are shown in Table 4. Minimum content of indium in the IBM is 17.07 wt.%, maximum – 19.41 wt.% (detection limit = 660 ppm) while arithmetic mean of measurements is 18.097 wt.% (geometric mean = 18.082 wt.%) and median 17.74 wt.%. Contents of Fe, Zn and Cu in the IBM vary and shows a general Zn>Cu>Fe proportion trend. Zn enrichment and a simultaneous decrease in Cu + Fe contents is noticeable. In comparison with the average chemical composition of sakuraiite (Table 1) there is a significant enrichment in Zn and a slight enrichment in Fe with depletion in Cu and In. Additionally, contents of Sn and Ag, found in an average formula in the range of 2–3 wt.%, in the IBM from Stara Kamienica, is at trace level. A spectrum of the indium-bearing mineral with visible indium peaks is shown in Figure 7.

In cases where In-rich sulphide forms intergrowths with chalcopyrite, both phases were measured (Fig. 6B). The results indicate that indium accumulates within the Zn-In-Cu-Fe sulphide admixture: points in chalcopyrite adjacent to this intergrowth show significant depletion in indium while farther away the indium content in the chalcopyrite increases. This probably represents a mixed phase of chalcopyrite and polymetallic indium-bearing mineral formed in the presence of various cations e.g. Cu, Zn, Fe, Ag and In. Figure 8 illustrates this situation: point 1, located directly within the indium-bearing mineral, contains 3.18 wt.% of In; point 2, located in the nearest area of the In-rich sulphide, contains a significantly reduced content of In (0.07 wt.%), while in points 3, 4, 5 and 6, as the distance from the indium phase intergrowth increases, the content of In also increases (Table 5).

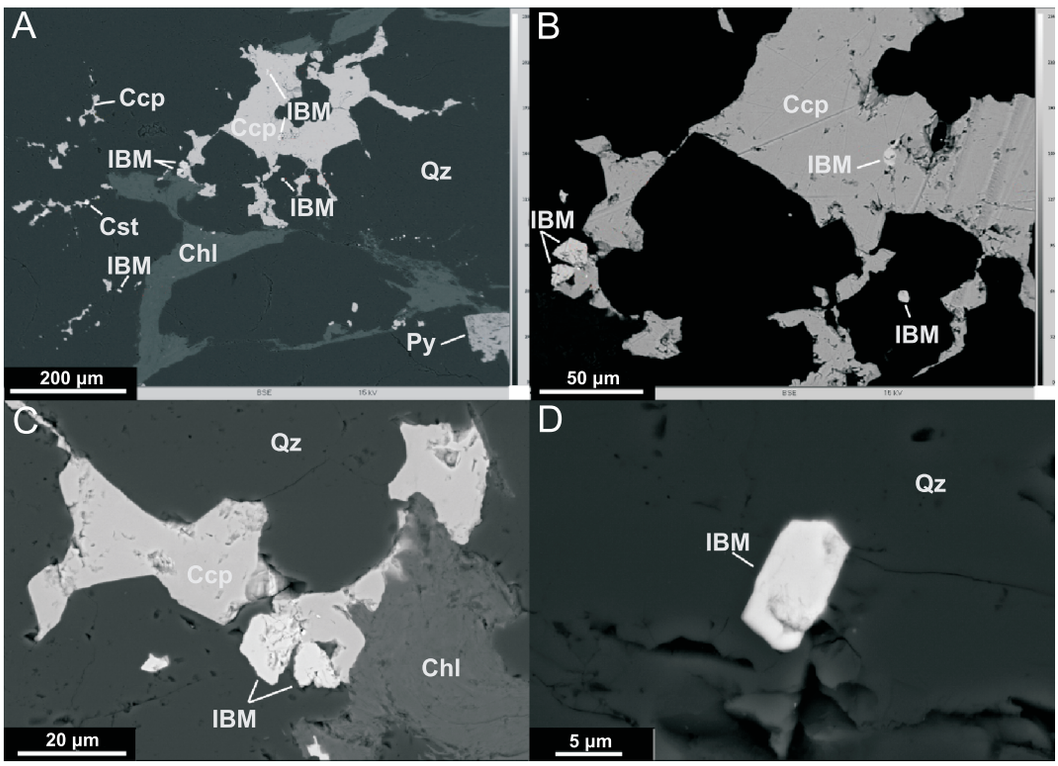

Fig. 6. Occurrence of the indium-bearing mineral

A, B – as intergrowths in chalcopyrite and separate grains;
C, **D** – cross-sectional surface morphology of IBM grains with visible hipautomorphic form within quartz, BSEI;
IBM – indium-bearing mineral, Ccp – chalcopyrite, Cst – cassiterite, Py – pyrite, Chl – chlorite, Qz – quartz

Table 4

EPMA results of the indium-bearing mineral hosted by cassiterite-sulphide mineralization in the Stara Kamienica Schist Belt in the Sudetes

Point#	S [wt.%]	Zn [wt.%]	In [wt.%]	Cu [wt.%]	Fe [wt.%]	Sn [ppm]	Si [ppm]	Cd [ppm]	Ga [ppm]	Co [ppm]	Total
1	30.43	33.68	17.52	9.14	8.13	640	2280	3950	b.d.l.	b.d.l.	99.77
2	29.39	30.83	18.61	10.56	8.86	590	1010	3600	b.d.l.	b.d.l.	98.96
3	29.78	29.76	19.41	10.75	8.62	720	950	3890	b.d.l.	b.d.l.	99.07
4	30.37	34.02	17.67	9.32	7.76	840	3140	3960	b.d.l.	b.d.l.	100.16
5	30.22	33.98	17.07	9.12	8.1	970	1730	3910	1260	b.d.l.	99.46
6	29.42	29.99	18.63	9.8	8.39	b.d.l.	2160	3840	b.d.l.	b.d.l.	96.99
7	30.77	31.66	17.77	9.05	8.7	590	3510	6610	b.d.l.	830	99.29
Average detection limit	0.02	0.13	0.05	0.10	0.05	421	241	583	1086	670	

Ag, Al, Ca, Sb, Cl, Bi, Pb, Se, As, Mg, Ba, Au, Te, Sb, Bi, Ni, and Mo below detection limits; b.d.l. – below detection limit

DISCUSSION

INDIUM CARRIERS

The presence of indium in the form of admixtures in chalcopyrite and sphalerite in the area studied has been reported previously and confirmed by the latest investigations (Piestrzyński and Mochnacka, 2003; Mikulski et al., 2018; Małek et al., 2019; Mikulski and Małek, 2019, Pietrzela, 2019, Foltyn et al., 2020). Elevated In contents in samples from the Stara Kamienica schists was first reported as traces in cassiterite by Wiszniewska (1984) and later by Piestrzyński and Mochnacka (2003) who, using the microprobe investigation method (Jeol 733), determined admixtures of indium in sphalerite (max. 1.39 wt.%) and stannite (max. 0.36 wt.%). Pietrzela (2019) noted the presence of indium in sphalerite (EMPA data) in the range of 0.05–0.11 wt.% and also in cassiterite in the range of

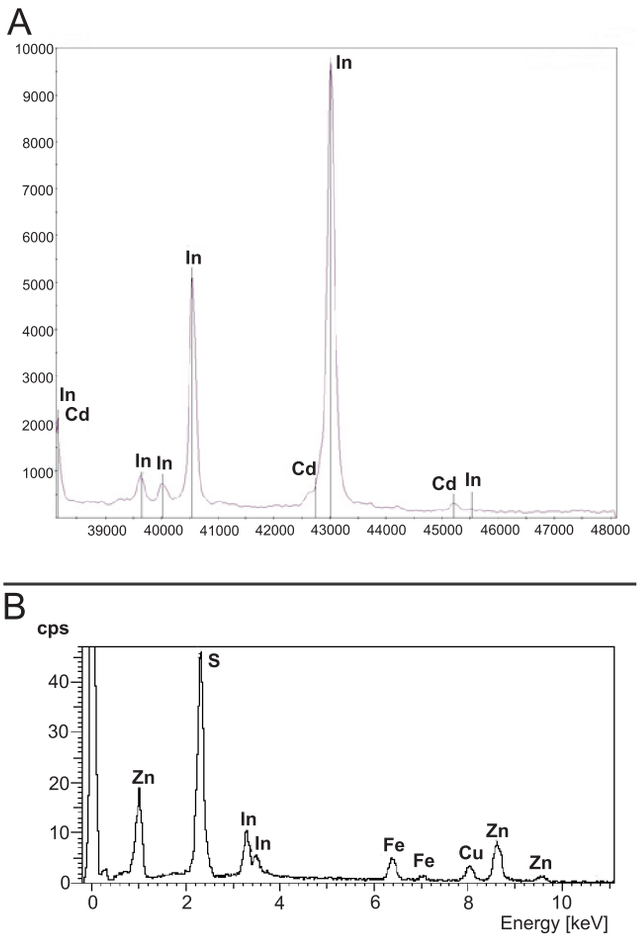

Fig. 7. Spectrum of the indium-bearing mineral

A – WDS (*Cameca SX-100*); **B** – EDS (*SEM Leo 1430*)

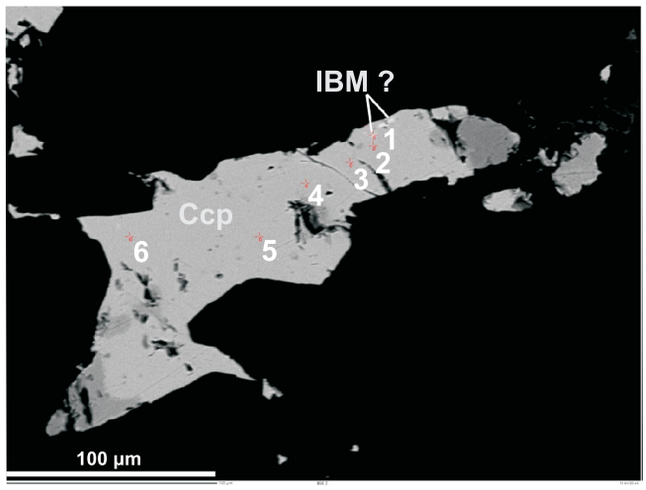

Fig. 8. Inclusions of the indium-bearing mineral mixture (IBM?) in chalcopyrite (Ccp); BSEI

1–6 – measurement WDS points

0.06–0.15 wt.%. Foltyn et al. (2020) indicated an average content of In (EMPA data) in sphalerite of 0.04 wt.%, in chalcopyrite of 0.01 wt.% (approx. to the detection limit) and in cassiterite of 0.01 wt.% (approx. to the detection limit). Our results of EMPA analysis of sphalerite for In content correspond to the results reported by other researchers. However, the average In content in chalcopyrite is three times higher than the average given by Foltyn et al. (2020). We have only performed EMPA test analyses for indium content in cassiterite and the results indicated values below detection limits.

A very rare indium mineral, sakuraiite, from the very moment of its first observation, creates problems of correct identification. It has been recognized in the Senju-hon vein located within Cretaceous rhyolitic and andesitic volcanic rocks of the Ikuno unit, Japan (Ichikawa et al., 1968). The vein showed a zonal structure and sakuraiite was found within a sakuraiite-stannite-cassiterite-sphalerite association (Kato, 1965). Kato (1965) concluded that sakuraiite was the indium equivalent of kesterite (Kissin and Owens, 1986) and because of that he described its structure as tetragonal. Kissin and Owens (1986) suggested a cubic structure of sakuraiite. This hypothesis seems to be consistent with their chemical composition results, which indicate a lack of stoichiometry in the atomic proportions of metals, suggesting that the metal sites in the structure are in equivalent positions (Kissin and Owens, 1986). The latest single-crystal X-Ray diffraction studies of Momma et al. (2017) reveal a pseudo-cubic crystal structure with a space group P-42m. Two non-equivalent sites in the sakuraiite structure were discovered. Cu, Zn and Fe atoms are randomly distributed in two crystallographic sites (1a and 2f), while In and Sn occur in another site (1d). Within each of these sites unlimited substitu-

Table 5

WDS results of the measurement points of the Zn-In-Cu-Fe sulphide from Figure 8

Point#	S [wt.%]	Zn [wt.%]	In [wt.%]	Cu [wt.%]	Fe [wt.%]	Sn [ppm]	Si [ppm]	Cd [ppm]	Co [ppm]	Total
1	31.46	33.02	3.18	16.36	15.01	1420	3820	2240	570	100.01
2	34.47	0.15	0.07	34.44	29.93	490	1110	b.d.l.	270	99.32
3	34.6	0.03	0.14	34.55	30.19	270	560	b.d.l.	440	99.85
4	34.53	0.15	0.13	34.62	30.03	b.d.l.	580	320	420	99.65
5	34.51	0.04	0.14	34.57	30.17	190	560	280	500	99.76
6	34.59	0.09	0.13	34.60	30.06	140	430	310	520	99.71

Ag, Al, Ca, Te, Sb, Cl, Ga, Bi, Ni, Mo, and Mg below detection limits; b.d.l. – below detection limit

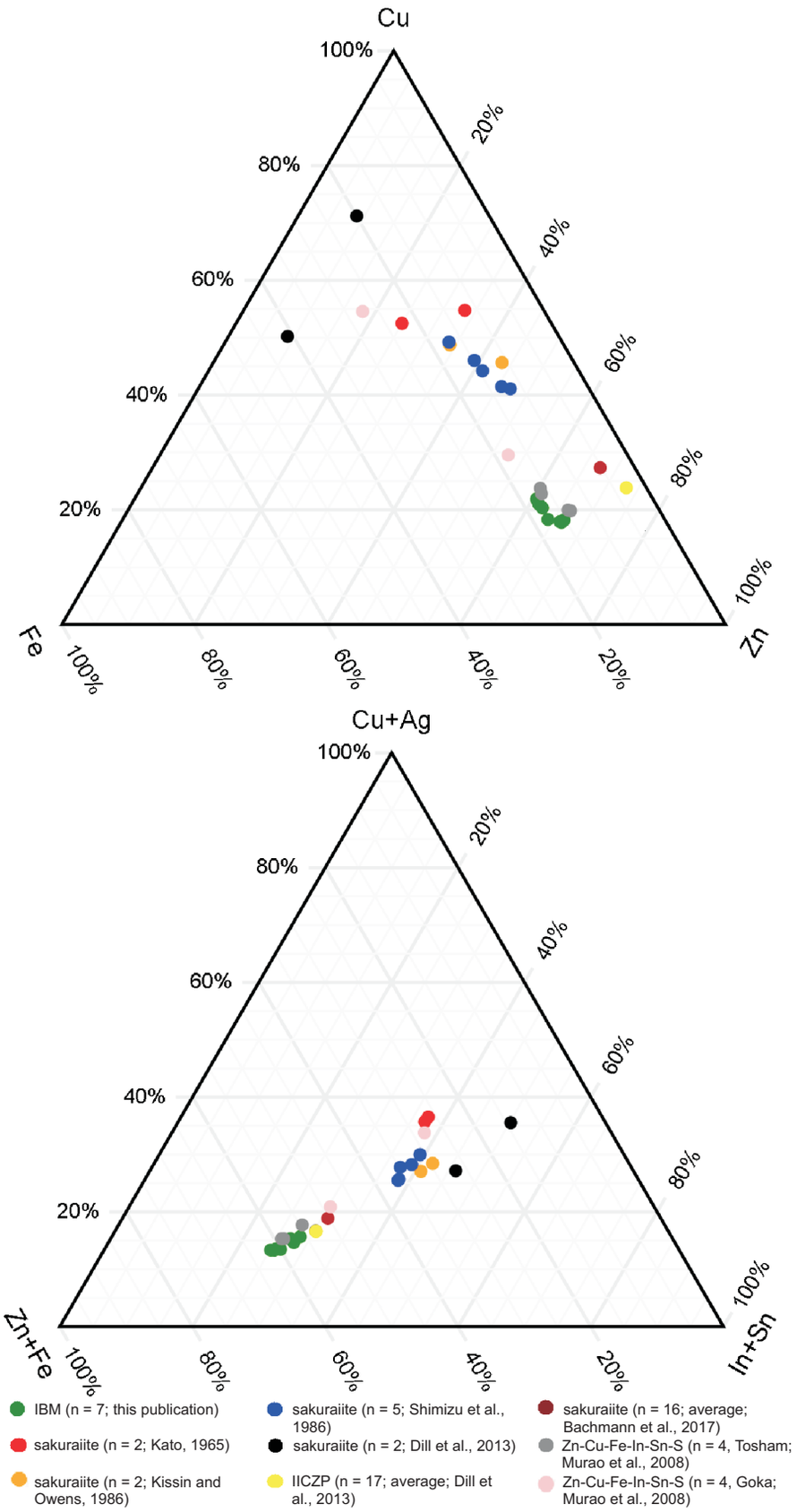

Fig. 9. Ternary plots of the chemical composition of sakuraiites and indium-bearing minerals obtained by different authors

tions of metals can occur, which explains the wide compositional range of this mineral.

Electron microbe analyses by Shimizu et al. (1986) of five sakuraiite grains showed that they are inhomogeneous in chemical composition. The measured contents of the elements display positive correlations between Zn, In and Cd, and negative for Cu and Zn (Shimizu et al., 1986). After fulfilment of the charge balance, assuming that Cu, Zn, Fe, Sn and In have the valencies 1 +, 2 +, 2 +, 4 + and 3 + respectively, as in stannite (Yamanaka and Kato, 1976; Nakai et al., 1978), the analyses yield an ideal sakuraiite formula of $(Cu,Zn,Fe,Ag)_3(In,Sn)S_4$. In addition, they assumed that two variants of the element proportions are possible: the first one is Cu>Zn>Fe + In>Sn and the second one is Zn>Cu>Fe + In>Sn.

Data obtained by us show similarities with the chemical composition of different sakuraiites and indium sulphide phases provided by other authors, and comparison of EMPA results reported by various researchers is shown in Figure 9 and Table 6. The main differences between the indium-bearing mineral from the Stara Kamienica Schist Belt and the sakuraiite analyses by Kato (1965), Shimizu et al. (1986), Kissin and Owens (1986) are:

- significant enrichment in Zn (~9–24 wt.%),
- significant depletion in Cu (~7–16 wt.%) and Sn (>1000 ppm *versus* 4–12 wt.%),
- significant depletion in Ag (>50 ppm *versus* 0.2 wt.%), especially in comparison with Kato's (1965) results (up to 4 wt.%).

Indium, iron and sulphur contents are, with small differences, at a similar level, as are trace contents of Cd (3000–8000 ppm).

Dill et al. (2013) report sakuraiite occurrence in the epithermal Au-Cu-Zn-Pb-Ag San Roque deposit (Argentina), where it has been observed as small intergrowths in single pyrite grains within a quartz matrix. Besides sakuraiite, roquesite and an unknown sulphide mineral named "Intermediate In-Cu-Zn Phase" (IICZP) have been identified as indium carriers. This unknown phase may be a mixture of indium-bearing minerals intergrown with each other and difficult to distinguish. The Zn-In-Cu-Fe sulphide described by us differs from the two sakuraiites reported from the San Roque deposit. The most significant difference is depletion in Cu (~8–16 wt.%), In (~8–11 wt.%), Sn (>1000 ppm *versus* 4–7 wt.%) and Ag (>100 *versus* 1700 ppm) with simultaneous enrichment in Zn (26–30 wt.%), The content of S (29–34 wt.%) and trace content of Cd (800–6000 ppm) are similar.

Results of EMPA studies in the indium-bearing mineral phase analyses defined by Dill et al. (2013) as an IICZP (n = 17) seems to be very similar to the results of the Zn-In-Cu-Fe sulphide reported in this publication. In both cases, the same Zn>Cu>Fe and In>Sn proportion of metal contents can be found. The average results obtained from 17 measurements of Zn, Cu, In and Sn content are similar to our results. A larger difference is present only in Fe content (average content in IICZP is lower, ~5–6 wt.%).

Sakuraiite was recognized within the Zn-Pb-Ag Santa Fe (Bolivia) deposit in the form of fine grains in association with stannite, cassiterite, sphalerite and galena. It contains a maximum 2.03 wt.% of indium and shows significant enrichment in Cu (21.68–27.54 wt.%) and Sn (18.30–26.67 wt.%) (Jiménez-Franco et al., 2018), which makes it significantly different from the indium-bearing phase described here.

The presence of a sakuraiite in the Chappara deposit in southern Peru was reported by Yáñez and Alfonso (2014). Sulphide mineralization is present in quartz veins within igneous rocks connected to the Coastal batholith. Sakuraiite occurs in association with galena, sphalerite and arsenopyrite as very small grains containing 5.43–6.41 wt.% of In (Yáñez and Alfonso, 2014).

A mineral called sakuraiite has been also reported from the Neves-Corvo mine (The Iberian Pyrite Belt, Portugal) by Bachmann et al. (2017). An average content from 16 EMPA

Table 6

Comparison of the EMPA results of sakuraiite and its unnamed indium-bearing mineral obtained by various authors

	S [wt.%]	Zn [wt.%]	Cu [wt.%]	In [wt.%]	Fe [wt.%]	Sn [wt.%]	Ag [wt.%]	Cd [wt.%]	Ga [wt.%]
Sakuraiite (n = 2; Kato, 1965)	30–31	10–14	21–23	17–23	5–9	4–9	3.5–4.0	–	–
Sakuraiite (n = 5; (Shimizu et al., 1986)	28.83–29.29	14.40–20.26	17.71–21.03	15.71–21.43	5.12–7.28	5.12–12.01	0.10–0.15	0.5–0.82	–
Sakuraiite (n = 2; Kissin and Owens, 1986)	29.0–29.1	13.7–18	18.9–19.6	22.0–23.8	4.5–6.9	4.9–7.2	0.1–0.2	0.6–0.7	–
Sakuraiite (n = 2; Dill et al., 2013)	30.90–33.53	3.11–3.34	18.83–25.07	27.96–28.25	7.03–15.33	4.20–7.37	0.14–0.17	0.08–0.18	0.89–1.45
IICZP (n = 17; Dill et al., 2013)	29.02–30.77	25.32–47.83	6.98–16.20	13.93–29.91	0.85–5.07	0.07–0.37	b.d.l.–0.04	0.27–0.35	b.d.l.
Sakuraiite (n = 16, averaged; Bachmann et al., 2017)	29.0	31.45	12.75	20.91	2.44	b.d.l.	b.d.l.	3.52	–
Zn-Cu-Fe-In-Sn-S (n = 4, Tosham; Murao et al., 2008)	29.4–30.9	29.1–34.3	10.2–12.0	18.0–21.0	6.9–8.1	b.d.l.	0.5–0.7	b.d.l.–0.2	–
Zn-Cu-Fe-In-Sn-S (n = 2, Goka; Murao et al., 2008)	29.7–30.6	7.9–25.4	14.3–23.9	8.8–19.8	8.7–12.0	1.4–18.1	b.d.l.–0.3	b.d.l.	–
IBM (n = 7; this publication)	29.39–30.77	29.76–34.02	9.05–10.75	17.07–19.41	7.76–8.86	b.d.l.–0.09	b.d.l.	0.36–0.40	b.d.l.–0.13

b.d.l. – below detection limit, IICZP – Intermediate In-Cu-Zn phase

measurements of this sakuraiite was: Cu – 12.75 wt.%, In – 20.91 wt.%, Zn – 31.45 wt.%, Fe – 2.44 wt.%, Cd – 3.52 wt.%, S – 29 wt.%, Ag and Sn below detection limit. The chemical composition of the indium-bearing mineral we describe is similar to the sakuraiite from Neves-Corvo, with the largest differences being an enrichment in Fe (7.76–8.86 wt.% *versus* 2.44 wt.%) and lower content of Cd (>4000 ppm *versus* 3.5 wt.%).

Murao et al. (2008) and Murao and Furuno (1990), described two different tin-polymetallic vein-type deposits with a similar ore mineralogy and chemistry. The first is the Tosham Sn-Cu deposit (Bhiwami district, India) with an unusually high content of indium. Disseminated, vein and stockwork mineralization is hosted by greisenised metasedimetary rocks which were intruded by a porphyrytic granite stock. The second is the Goka deposit (Naegi district, Japan) which represents tin-polymetallic vein-type mineralization hosted by welded tuffs which are close to a subvolcanic granodiorite porphyry. In both deposits the main indium hosts are sphalerite, stannite, chalcopyrite and unidentified Zn-Cu-Fe-In-Sn-S phases. Representative analyses of In-bearing phases from the Tosham and Goka deposits are shown in Table 6.

Sakuraiite has been also recognized in two localities in Russia (Alekseev and Marin, 2015; Damdinova et al., 2019), however, the authors do not provide EPMA results.

Ternary plots (Fig. 9) indicate that the Zn-In-Cu-Fe sulphide we describe shows a great resemblance to the IICZP from the San Roque deposit (Dill et al., 2013), the mineral called sakuraiite from the Neves-Corvo mine (Bachmann et al., 2017) and the Zn-Cu-Fe-In-Sn-S mineral phase from the Tosham and Goka deposits (Murao et al., 2008).

Based on average EMPA results, the empirical formula of the indium mineral phase from the Stara Kamienica Schist Belt has been established – $(Zn_{2.09}In_{0.67}Cu_{0.65}Fe_{0.64}Cd_{0.02})_{\Sigma 4.07}S_{4.0}$. This formula is significantly different from the sakuraiite formula given by Kato (1965) as $(Cu_{1.41}Zn_{0.92}In_{0.86}Fe_{0.38}Sn_{0.14}Ag_{0.14})_{\Sigma 3.85}S_{4.00}$ and later by Fleischer (1968) as $(Cu_{1.36}Zn_{0.92}In_{0.84}Fe_{0.54}Sn_{0.27}Cd_{0.02}Ag_{0.01})_{\Sigma 3.96}S_{4.00}$ (after Anthony et al., 1990). Shimizu et al. (1986) calculated the following formula of sakuraiite: $(Cu_{1.32}Zn_{1.22}In_{0.92}Fe_{0.36}Sn_{0.18}Cd_{0.03})_{\Sigma 4.03}S_{4.00}$. The main differences are in the proportions of individual components; especially significant is the more than doubled enrichment in Zn compared to other cations and corresponding depletion in Cu. Compared to Kato (1965), the difference in S deficiency relative to cations is notable, while in the formula given by Shimizu et al. (1986) there is also an excess of cations. Murao et al. (2008) provide formulae of the representative analyses of In-bearing phases from both the Tosham and Goka occurrences. The average calculated formula of the Zn-Cu-Fe-In-Sn-S mineral from the Tosham deposit is $(Zn_{0.52}Fe_{0.14}Cu_{0.18}In_{0.18})S_{0.98}$ while from the Goka deposit it is $(Zn_{0.27}Fe_{0.19}Sn_{0.08}Cu_{0.40}In_{0.13})S$. In spite of the fact that these formulae were calculated to one sulphur atom, the similarity between the mineral from the Stara Kamienica Schist Belt and from the Tosham occurrence is clear. A more significant difference was observed in the case of the Goka mineral phase due to its higher Sn and lower Zn proportion. Neither Dill et al. (2013) nor Bachmann et al. (2017) provide empirical formulae of their indium-bearing minerals. Details of establishing the empirical formula for the Zn-In-Cu-Fe sulphide are shown in Table 7.

INDIUM EVENT IN AN ORE-MINERAL SUCCESSION

The genesis of tin and base metal (cassiterite-sulphide) mineralization is related to the activity of hydrothermal solutions closely linked with the evolution of the Izera metamorphic complex, but interpretations differ. For example, according to Wiszniewska (1984), the genesis of the tin-sulphide mineralization is genetically linked directly to the intrusion of the Variscan Karkonosze Granitoid Massif (magmatic emplacement ~320–300 Ma), but earlier development of magmatic-metamorphic processes (Michniewicz et al., 2006) as well as pre- and syn-Variscan multiple mineralization events have also been proposed (Cook and Dudek, 1993; Mikulski et al., 2007). Numerous studies of garnets, which are accessory in tin-bearing schists, and especially of inclusions in cassiterites and ilmenites, as well as the zonation of metamorphic garnets themselves, may indicate a hydrothermal and post-metamorphic genesis of cassiterite mineralization (Kozłowski et al., 1988; Wiszniewska et al., 1998). On the other hand, Cook and Dudek (1994) correlated the formation of at least part of the polymetallic (Co-Ni-As-Bi-Ag) sulphide mineralization with one of the phases of high-temperature regional metamorphism (~400–340 Ma). There are also a number of studies suggesting the sedimentary pre-metamorphic (syngenetic) genesis of the cassiterite mineralization (i.e. Szałamacha, 1976). Some of the researchers (e.g., Piestrzyński and Mochnacka, 2003), as well as the authors of this article, support a more complex metasomatic-hydrothermal genesis connected with multi-stage development of intrusive-metamorphic processes of pre-, syn- and post-Variscan events (Mikulski et al., 2007).

The unnamed Zn-In-Cu-Fe sulphide described here is genetically connected with indium-bearing chalcopyrite, because its only observed occurrences are intergrowths in chalcopyrite, aggregates with chalcopyrite and separate grains in the immediate vicinity of chalcopyrites.

Analyses of mutual mineral relations indicate that sphalerites and chalcopyrites, which later researchers determined as carriers of trace indium admixtures (Piestrzyński and Mochnacka, 2003; Mikulski et al., 2018; Małek and Mikulski, 2019; Foltyn et al., 2020) crystallized together. In the ore mineral succession they represent the late stage of high and medium temperature (550–250°C) events of the epigenetic miner-

Table 7

Averaged contents of individual components in the empirical formula of the Zn-In-Cu-Fe sulphide

	Atomic [%]								
	S	In	Cd	Ga	Zn	Cu	Sn	Fe	Total
Average (n = 7)	49.30	8.29	0.20	0.05	25.72	8.02	0.03	7.88	99.48
Normalized to 100%	49.56	8.34	0.20	0.05	25.85	8.06	0.03	7.92	100.00
Normalized to 4 sulphur atoms	4.00	0.67	0.02	0.00	2.09	0.65	0.00	0.64	8.07

alization (postmagmatic-hydrothermal; Wiszniewska, 1984; Wiszniewska et al., 1998). It is considered that tin mineralization crystallized in two stages: cassiterites of the first generation (1st) crystallized at the beginning of the high temperature stage (460–420°C) while later cassiterites of the second generation (2nd) crystallized simultaneously with sulphides (365–325°C; Wiszniewska et al., 1998). Studies based on an arsenopyrite thermometer carried out by Cook and Dudek (1994) to determine P/T conditions of sulphide mineralization in the Stara Kamienica area indicates, depending on the parageneses analysed, temperatures of 430–448°C, 463°C and 508–517°C and P/T conditions for the crystallization of sphalerites accompanying the cassiterites at 550–500°C and 6.0–7.5 kbar. Foltyn et al. (2020), though, determined the crystallization temperatures of indium-bearing sphalerites at 349–331°C.

A costibite mineral accompanying chalcopyrite and sphalerite appears to be the low-temperature polymorph of CoSbS (Cabri et al., 1970); the presence of bastnäsite also indicates lower crystallization temperatures (it is stable only in greenschist facies; Savko and Bazikov, 2011). The sphalerite, on the other hand, containing an average of 8.1 wt.% Fe, indicates high crystallization temperatures (Cook and Dudek, 1994).

The indium-bearing chalcopyrite with which the indium mineral phase is associated seems to belong to the main generation of chalcopyrite, defined by Wiszniewska (1984) as chalcopyrite 2nd. In addition, this is supported by the proximity of cassiterite 2nd generation and pyrite (Fig. 6A) and similarly by the sulphosalts which also occur as intergrowths in chalcopyrite (Wiszniewska, 1984). Taking into account a genetic connection between the indium mineral phase and chalcopyrite 2nd, we can assume that their P/T crystallization conditions are similar and correspond with the middle and high temperature stage of the sulphide succession. At this stage of mineral crystallization successions there are cassiterite 1st, pyrrhotite, arsenopyrite, cobaltite, loellingite, safflorite, native bismuth, magnetite, pyrite, sphalerite, chalcopyrite 2nd, cassiterite 2nd, galena (Bi-bearing), bismuthinite, galenobismuthite and cosalite (Wiszniewska, 1984; Speczik and Wiszniewska, 1984). A very similar polymetallic sulphide association (with subordinate cassiterite) has been described in the east metamorphic cover of the Karkonosze Granite Massif where, in the abandoned Czarnów As-polymetallic deposit, isotopic Re-Os investigation indicated arsenopyrite crystallization at 312 ±3 Ma (Mikulski and Stein, 2011).

Indium-bearing mineralization is often connected to and developed in or around volcano-plutonic complexes, especially in transitional zones between the Sn-bearing and epithermal zones (Murao, 2008; Dill et al., 2013). There are many examples worldwide: the Toyoha deposit (Japan) where In-bearing polymetallic mineralization is located in a transitional zone between the products of I-type magmatism and the epithermal zone (Ohta, 1989, 1995); the Tigrinoe deposit (Russia) where Sn-sulphide vein mineralization is connected to the Zinnwaldite granite-porphyry complex and monzonite Burelomny stock (Pavlova et al., 2015), the Pravourmiiskoe deposit (Russia) where a genetic link between indium-bearing Sn mineralization and granite of the Verhneurmiisky pluton is widely inferred; the Tosham deposit (India) where Sn-Cu mineralization with a high indium content is hosted by greisenised metasedimentary rocks intruded by a porphyritic granite stock and rhyolitic effusive rocks (Murao et al., 2008). The Karkonosze granite massif seems to correspond to this volcano-plutonic indium-bearing Sn-sulphide environment. This similarity may provide another clue that the cassiterite-sulphide mineralization stage with indium enrichment at Stara Kamienica is genetically linked with the presence and hydrothermal activity of the Karkonosze granite. Karkonosze pluton magmas are strongly evolved and fractionated, making them a potential source of metals such as Mo-W-Sn-Fe-Cu-REE-Nb-Y-U-Th (Mikulski, 2007). Within the Karkonosze pluton and its near vicinity much sulphide mineralization comprising Mo-W-Sn-Bi-Fe-Cu associations occur that were genetically related to the pluton (Mochnacka et al., 2015 with references therein; Mikulski et al., 2020b).

CONCLUSIONS

– Based on EMPA studies, an unnamed indium-bearing mineral (Zn-In-Cu-Fe sulphide) has been recognized in samples from the stratiform tin deposit of the Stara Kamienica schist belt (Sudetes). This mineral contains up to 19.41 wt.% of In and has the following empirical formula: $(Zn_{2.09}In_{0.67}Cu_{0.65}Fe_{0.64}Cd_{0.02})_{?4,07}S_{4,0}$.

– This indium-bearing mineral differs from sakuraiite in the proportion of individual cations, having more than double enrichment in Zn, more than double depletion in Cu and a very low Sn content. The range of the metal proportions and contents in the Zn-In-Cu-Fe sulphide investigated from the Stara Kamienica area indicates significant similarity to unnamed In-Cu-Zn phase described from San Roque (Argentina) (Dill et al., 2013), an unidentified Zn-Cu-Fe-In-Sn-S mineral from the Tosham deposit (India) and the Goka deposit (Japan; Murao et al., 2008) and also to the mineral called “sakuraiite” from the Neves-Corvo mine (Portugal) described by Bachmann et al. (2017). In all these cases, significant enrichments in Zn relative to the rest of the cations were found, as well as low (trace) contents of Sn and Ag and a measured Cd content at level above the detection limit.

– The Zn-In-Cu-Fe sulphide described is genetically linked with the main generations of chalcopyrite and sphalerite in the sulphide succession, the formation of which is associated with medium and high temperature postmagmatic-hydrothermal mineralization, most likely after the intrusion of the Karkonosze granite.

– In addition, EPMA measurements identified admixtures of indium in sphalerites and chalcopyrites, which have already been described in the case of cassiterite-sulphide mineralization from the Stara Kamienica schist belt in the Sudetes.

– Other examples of indium-bearing mineralization worldwide connected with volcano-plutonic complexes may emphasise the genetic link between the Stara Kamienica Sn-sulphide mineralization and the Karkonosze granite pluton.

Acknowledgements. We are grateful to the reviewers K. Foltyn and J. Janeczek for their constructive reviews and valuable suggestions that greatly improved the first version of the manuscript. This work was financially supported by the European Union’s Horizon 2020 research and innovation programme under grant agreement no. 731166. Scientific work was co-funded by national funds allocated for science within the period 2018–2021 under grant agreement 4091/H2020/2018/2 and by the Polish Geological Institute – National Research Institute through an internal grant no. 61.2905.1802.00.0. for S.M.

REFERENCES

Alekseev, V.I., Marin, Y.B., 2015. Composition and evolution of accessory mineralization of Li–F granites in the Far East as indicators of their ore potential. Geology of Ore Deposits, **57**: 635–644.

Anderson, C.S., 2020. Indium. In: Mineral Commodity Summaries 2020: 78–79. United States Geological Survey.

Anthony, J.W., Bideaux, R.A., Bladh, K.W., Nichols, M.C., 1990. Handbook of Mineralogy (**I** – Elements, Sulfides, Sulfosalts): Mineral Data Publishing, Tucson, Arizona http://www.handbookofmineralogy.com/pdfs/sakuraiite.pdf .

Bachmann, K., Frenzel, M., Krause, J., Gutzmer, J., 2017. Advanced identification and quantification of In-bearing minerals by scanning electron microscope-based image analysis. Microscopy and Microanalysis, **23**: 527–537.

Barbalace, K., 2019. Periodic Table of Elements. EnvironmentalChemistry.com

Berendsen, P., Speczik, S., Wiszniewska, J., 1987. Sulphide geochemical studies of the stratiform tin deposits in the Stara Kamienica Chain (SW Poland). Archiwum Mineralogiczne, **42**: 31–42.

Bobiński, W., 1991. Wrostki kasyterytu w minerałach skałotwórczych (in Polish). In: Mineralizacja Sn i jej pozycja w ewolucji geologicznej pasma Kamienieckiego (Góry Izerskie – Sudety Zachodnie). Materiały CXXXI Sesji Nauk PIG: 4–5.VI.1991. Wrocław.

Cabri, L.J., Harris, D.C., Stewart, J.M., 1970. Costibite (CoSbS), a new mineral from Broken Hill, N.S.W., Australia. American Mineralogist, **55**: 10–17.

Cantinolle, P., Laforet, C., Maurel, C., Picot, P., Grangeon, I.J., 1985. Contribution a la mineralogy de l'indium. Decouverte en France de deux nouveaux sulfures d'indium de deux nouvelles occurrences de roquesite. Bulletin de Minéralogie: Mineral Cristallographie, **108**: 245–248.

Cook, N.J., Dudek, K., 1994. Mineral chemistry and metamorphism of garnet chlorite–mica schist associated with cassiterite–sulphide mineralization from the Kamienica Range, Izera Mountains, S.W. Poland. Chemie der Erde, **54**: 1–32.

Damdinova, L.B., Damdinov, B.B., Huang, X.W., Bryansky, N.V., Khubanov, V.B., Yudin, D.S., 2019. Age, conditions of formation, and fluid composition of the Pervomaiskoe molybdenum deposit (Dzhidinskoe ore field, south-western Transbaikalia, Russia). Minerals, **9**: 572.

Dill, H.G., 2010. The "chessboard" classification scheme of mineral deposits: mineralogy and geology from aluminum to zirconium. Earth-Science Reviews, **100**: 1–420.

Dill, H.G., Garrido, M.M., Melcher, F., Gomez, M.C., Weber, B., Luna, L.I., Bahr, A., 2013. Sulfidic and non-sulfidic indium mineralization of the epithermal Au-Cu-Zn-Pb-Ag deposit San Roque (Provincia Rio Negro, SE Argentina) – with special reference to the "indium window" in zinc sulphide. Ore Geology Reviews, **51**: 103–128.

Fleischer, M., 1968. New mineral names. American Mineralogist: 53: 1421.

Frenzel, M., Hirsch, T., Gutzmer, J., 2016. Gallium, germanium, indium, and other trace and minor elements in sphalerite as a function of deposit type – a meta-analysis. Ore Geology Reviews, **76:** 52–78.

Foltyn, K., Bertrandsson Erlandsson, V., Kozub-Budzyń, G.A., Melcher, F., Piestrzyński, A., 2020. Indium in polymetallic mineralisation at the Gierczyn mine, Karkonosze-Izera Massif, Poland: results of EPMA and LA-ICP-MS investigations. Geological Quarterly, **64** (1): 74–85.

Genkin, A.D., Murav'eva, I.V., 1963. Novyye mineral indiya (in Russian). Zapiski Vsesoyuznogo Mineralogicheskogo Obshchestva, **92:** 445.

Ichikawa, K., Murakami, N., Hase, A., Wadatsumi, K., 1968. Late Mesozoic igneous activity in the Inner Side of Southwest Japan. Pacific Geology, **1**: 97–118.

Ivanov, V.V., 1963. Indium in some igneous rocks of the USSR. Geochemistry, **12**: 1–15.

Jiménez-Franco, A., Alfonso Abella, M.P., Canet Miquel, C., Trujillo, J.E., 2018. Mineral chemistry of In-bearing minerals in the Santa Fe mining district, Bolivia. Andean Geology, **45**: 410–432.

Jorgenson, J.D., George, M.W., 2005. Mineral Commodity Profile: Indium. U.S. Geological Survey Open-File Report 2004–1300.

Kato, A., 1965. Sakuraiite, a new mineral (in Japanese). Chigaku Kenkyu, Sakurai Volume: **1**–**5.**

Kissin, S.A., Owens, D.R., 1986. The crystallography of sakuraiite. Canadian Mineralogist, **24:** 679–683.

Kooiman, G.J.A., Ruitenberg, A.A., 1992. Indium deposits and their economic potential: report on a mission to Japan. New Brunswick Department of Natural Resources and Energy, Mineral Resources, Geoscience Report, 92–3.

Kowalski, W., Karwowski, Ł., Śmietańska, I., Do Van Phi., 1978. Ore mineralization of the Stara Kamienica Schist Belt in the Izera Mountains (in Polish with English summary). Prace Naukowe Uniwersytetu Śląskiego, **243**: 7–89.

Kozłowski, A., Wiszniewska, J., Metz, P., 1988. Garnet-bearing parageneses of the tin deposits in the Stara Kamienica Chain, Lower Silesia. Fortschritte der Mineralogie, **66**: 85–86.

Kucha, H., Mochnacka, K., 1987. Preliminary report on bismuth minerals from the Gierczyn tin deposit, Lower Silesia, Poland. Mineralogica Polonica, **17**: 55–61.

Lokanc, M., Eggert, R., Redlinger, M., 2015. The Availability of Indium: the Present, Medium Term, and Long Term, National Renewable Energy Laboratory (NREL) report (https://www.nrel.gov/docs/fy16osti/62409.pdf).

Małek, R., Mikulski, S.Z., 2019. Geochemical-mineralogical research of the rare and associated element concentrations within cassiterite-sulphide mineralization in the Stara Kamienica schist belt in the Western Sudetes – preliminary results (in Polish with English summary). Przegląd Geologiczny, **67**: 179–182.

Małek, R., Mikulski, S.Z., Chmielewski, A., 2019. The geochemical-mineralogical characteristic of cassiterite-sulphide mineralization in the historic Saint John and Saint Leopold shafts in the Stara Kamienica schist belt (Western Sudetes) (in Polish with English summary). Przegląd Geologiczny, **67**: 910–920.

Mazur, S., Aleksandrowski, P., Kryza, R., Oberc-Dziedzic, T., 2006. The Variscan orogen in Poland. Geological Quarterly, **50** (1): 89–118.

Michniewicz, M., Bobiński, W., Siemiątkowski, J., 2006. Tin mineralization in the middle part of the Stara Kamienica Schist Belt (Western Sudetes) (in Polish with English summary). Prace Państwowego Instytutu Geologicznego, **186:** 1–137.

Mikulski, S.Z., 2007. Metal ore potential of the parent magma of granite – the Karkonosze massif example. Archivum Mineralogiae Monograph, **1**: 123–145.

Mikulski, S.Z., Małek, R., 2019. Indium and other critical elements enrichment in cassiterite-sulphide mineralization from the stratiform tin deposits in the West Sudetes (SW Poland). 15th SGA Biennial Meeting, 27–30 August 2019, Glasgow, Scotland, **4:** 1818–1821.

Mikulski, S.Z., Stein, H.J., 2011. Re-Os age for molybdenite from the Variscan Karkonosze massif and its eastern metamorphic cover (SW Poland). Proceedings of the 11th SGA Biennial Meeting, Antofagasta, 130–133. Ediciones Universidad Católica del Norte; Antofagasta.

Mikulski, S.Z., Kozłowski, A., Speczik, S., 2007. Fluid inclusion study of gold-bearing quartz-sulphide veins and cassiterite from the Czarnow As deposit ore (SW Poland). Proceedings of the Ninth Biennial SGA Meeting, Dublin 2007: 805–808.

Mikulski, S.Z., Oszczepalski, S., Sadłowska, K., Chmielewski, A., Małek, R., 2018. The occurrence of associated and critical elements in the selected documented Zn-Pb, Cu-Ag, Fe-Ti-V, Mo-Cu-W, Sn, Au-As and Ni deposits in Poland (in Polish with

English summary). Biuletyn Państwowego Instytutu Geologicznego, **472**: 21–52.

Mikulski, S.Z., Oszczepalski, S., Sadłowska, K., Chmielewski, A., Małek, R., 2020a. Trace element distributions in the Zn-Pb (Mississippi valley-type) and Cu-Ag (Kupferschiefer) sediment-hosted deposits in Poland. Minerals, **10**: 1–47.

Mikulski, S.Z., Williams, I.S., Stein, H.J., Wierchowiec, J., 2020b. Zircon U-Pb Dating of Magmatism and Mineralizing Hydrothermal Activity in the Variscan Karkonosze Massif and Its Eastern Metamorphic Cover (SW Poland). Minerals, **10**: 787

Mochnacka, K., 1986. Structures and textures of ores from the Gierczyn tin ore deposit (Sudetes, Poland) and their genetic interpretation. Mineralogica Polonica, **16**: 85–96.

Mochnacka, K., Oberc-Dziedzic, T., Mayera, W., Pieczka, A., 2015. Ore mineralization related to geological evolution of the Karkonosze–Izera Massif (the Sudetes, Poland) – towards a model. Ore Geology Reviews, **64**: 215–238.

Momma, K., Miyawaki, R., Matsubara, S., Shigeoka, M., Nagase, T., Kamada, S., Ozawa, S., Ohtani, E., Shimizu, M., Kato, A., 2017. The crystal chemistry of sakuraiite. Acta Crystallographica Section A: Foundations and Advances, **73:** 910.

Murao, S., Furuno, M., 1990. Indium-Bearing Ore from the Goka Mine Naegi District, Southwestern Japan. Mining Geology, **40**: 35–42.

Murao, S., Deb, M., Furuno, M., 2008. Mineralogical evolution of indium in high grade tin-polymetallic hydrothermal veins – a comparative study from Tosham, Haryana state, India and Goka, Naegi district, Japan. Ore Geology Reviews, **33:** 490–504.

Nakai, I., Sugitani, Y., Nagashima, K., Niwa, Y., 1978. X-ray photoelectron spectroscopic study of copper minerals. Journal of Inorganic and Nuclear Chemistry, **40:** 789–791.

Nechayev, I., 1987. Native indium and Fe in tin-bearing greisens of the Ukrainian Shield (in Russian with English summary). Mineralogicheskiy Zhurnal, **9**: 74–78.

Ohta, E., 1989. Occurrence and chemistry of indium-containing minerals from the Toyoha mine, Hokkaido, Japan. Mining Geology, **36**: 355–372.

Ohta, E., 1995. Common features and genesis of tin-polymetallic veins. Resource Geology Special Issue, **18**: 187–195.

Pavlova, G.G., Palessky, S.V., Borisenko, A.S., Vladimirov, A.G., Seifert, T., Luu Anh, P., 2015. Indium in cassiterite and ores of tin deposits. Ore Geology Reviews, **66**: 99–113.

Picot, P., Pierrot, R., 1963. La roquesite, premier mineral d'indium. Bulletin de Minéralogie: Mineral Cristallographie, **86**: 7–14.

Piestrzyński, A., Mochnacka, K., 2003. Discussion on the sulphide mineralization related to the tin-bearing zones of the Kamienica schist belt Western Sudety Mountains, SW (in Polish with English summary). In: Sudety Zachodnie od wendu do czwartorzędu (eds. W. Ciężkowski, J. Wojewoda and A. Żelaźniewicz): 169–182. WIND, Wrocław.

Piestrzyński, A., Mochnacka, K., Mayer, W., Kucha, H., 1990. Scheelite and ferberite from the tin-bearing schists of the Kamienica Range (the Sudetes, SW Poland). Mineralogica Polonica, **21**: 5–14.

Piestrzyński, A., Mochnacka, K., Mayer, W., Kucha, H., 1992. Native gold (electrum), Fe-Co-Ni arsenides and sulphoarsenides in the mica schists from Przecznica, the Kamienica Range, SW Poland. Mineralogica Polonica, **23**: 27–43.

Pietrzela, A., 2019. Reassessment of Sn-Co mineralization in mica schists of the Krobica-Gierczyn area (SW Poland). 15th SGA Biennial Meeting, 27–30 August 2019, Glasgow, Scotland, 4: 1454–1457.

Sahlström, F., Arribas, A., Dirks, P., Corral, I., Chang, Z., 2017. Mineralogical distribution of germanium, gallium and indium at the Mt Carlton high-sulfidation epithermal deposit, NE Australia, and comparison with similar deposits worldwide. Minerals, **7**: 1–28.

Savko, K.A., Bazikov, N.S., 2011. Phase equilibria of bastnaesite, allanite and monazite: bastnaesite-out isograde in metapelites of the Vorontsovskaya Group, Voronezh Crystalline Masiff. Petrology, **19**: 445–469.

Schwarz-Schampera, U., 2014. Indium. In: Critical Metals Handbook (ed. G. Gunn). Wiley-Blackwell, London.

Schwarz-Schampera, U., Herzig, P.M., 2002. Indium. Geology, Mineralogy, and Economics. Springer, Berlin.

Shimizu, M., Kato, A., Shiozawa, T., 1986. Sakuraiite: chemical composition and extent of (Zn,Fe)In-for-CuSn substitution. Canadian Mineralogist, **24**: 405–410.

Smulikowski, W., 1972. Petrogenetic and structural problems of the northern cover of the Karkonosze Granite (in Polish with English summary). Geologica Sudetica, **6:** 97–188.

Speczik, S., Wiszniewska, J., 1984. Some comments about stratiform tin deposits in the Stara Kamienica Chain (southwestern Poland). Mineralium Deposita, **19**: 171–175.

Stevens, L.G., White, C.E.T., 1990. Indium and Bismuth. Metals Handbook, **2**, ASM International, USA.

Szałamacha, M., 1976. On the origin of cassiterite mineralization in the metamorphic schists of the Karkonosze-Góry Izerskie (Mts.) Block, the Sudetes. In: The Current Metallogenic Problems of Central Europe (ed. J. Fedak): 343–349. Wyd. Geol., Warszawa.

Szałamacha, M., Szałamacha, J., 1974. Geological and petrographic characteristic of schists mineralized with cassiterite on the basis of materials from the quarry at Krobica (in Polish with English summary). Biuletyn Państwowego Instytutu Geologicznego, **279**: 59–89.

Taylor, S.R., McLennan, S.M., 1985. The continental crust: its composition and evolution. The Materials Information Society, Ohio.

Torró, L., Melgarejo, J.C., Gemmrich, L., Mollinedo, D., Cazorla, M., Martínez, Á., Pujol-Solà, N., Farré-de-Pablo, J., Camprubí, A., Artiaga, D., Torres, B., Alfonso, P., Arce, O., 2019. Spatial and temporal controls on the distribution of indium in xenothermal vein-deposits: the Huari Huari district, Potosí, Bolivia. Minerals, **9**: 304.

Wager, L.R., van Smit, R., Irving, H., 1958. Indium content of rocks and minerals from the Skaergaard intrusion, East Greenland. Geochimica et Cosmochimica Acta, **13**: 81–86.

Wiszniewska, J., 1983. Origin of tin mineralization of the Izera schists in Kamienieckie Range (Sudetes). Archiwum Mineralogiczne, **38**: 45–55.

Wiszniewska, J., 1984. The genesis of ore-mineralization of the Izera schists in the Kamienieckie Range (Sudetes) (in Polish with English summary). Archiwum Mineralogiczne, **40**: 115–187.

Wiszniewska, J., Kozłowski, A., Metz, P., 1998. Significance of the composition of garnet to clarify the origin of tin mineralization in the Stara Kamienica schist belt, southwest Poland. Proc. of IX-th Qadrennial Symp. IAGOD Beijing, China, Stuttgart: 463–473.

Yamanaka, T., Kato, A., 1976. Mossbauer effect study of ^{57}Fe and ^{119}Sn in stannite, stannoidite and mawsonite. American Mineralogist, **61**: 260–265.

Yáñez, J., Alfonso, P., 2014. Mineralogy of the Chaparra IOCG deposit, southern Peru. In EGU General Assembly Conference Abstracts, **16**: https://meetingorganizer.copernicus.org/EGU2014/EGU2014-15675.pdf